SUPPLEMENTARY MATERIALS

Visual Saliency Computations: Mechanisms, Constraints, and the Effect of Feedback

Alireza Soltani[1,2] and Christof Koch[1]
[1]Division of Biology and Computation and Neural Systems
California Institute of Technology, Pasadena, CA 91125
[2]Baylor College of Medicine, Houston, TX 77030

July 9, 2010

In the following sections we provide some additional details about the spiking network model as well as some results which are of interest to the reader.

A global measure of saliency signals

In order to define a global measure of saliency which can be compared to the local popout selectivity index (PI), we use the difference in the global saliency indices (GSI, see Methods for the definition) between popout and conjunction displays. More specifically, we define the *global popout selectivity index* (GPI) for a given popout display to be equal to the difference between the global saliency index for that popout (GSI_{popout}) and conjunction (GSI_{conj}) divided by their sum

$$GPI = \frac{GSI_{popout} - GSI_{conj}}{GSI_{popout} + GSI_{conj}} \,. \tag{S1}$$

GPI quantifies the ability of a population of neurons to detect a target in popout displays versus in the conjunction display, and increases in higher areas for configuration A (Fig. S4C and Fig. S5).

Interestingly, we find a strong correlation between PI and GPI in both configurations (Fig. S4C and Fig. S5). This indicates that both local and global popout selectivity indices can be equally informative about the saliency of the target. We conclude that even though global saliency indices are more proper measures of saliency signals, local measures of saliency such as popout selectivity indices, measured in electrophysiological recording, also provide accurate information about the saliency computations.

Additional tables and figures

Table 1 and Table 2 provides all details about the strength and form of connectivity between neurons in different layers of the network and for two sets of simulations presented in the main paper, respectively.

In brief, Fig. S1 shows different stimuli which we use to generate the inputs to our network. These stimuli are similar to ones used in the monkey experiment [1]. In Fig.S2 we present the average response to different visual stimuli in successive layers of the network. Fig. S3 to Fig. S7 provide more

information on how local and global saliency signals evolve in successive layers of the network for two different configurations. Fig. S8 to Fig. S10 show how increasing the AMPA to NMDA current ratio deteriorates the formation of saliency signals in successive layers of the network. At the end, Fig. S11 shows the response of neurons selective to the target (black) and distractors (gray) in the saliency map, to different displays and under three different conditions.

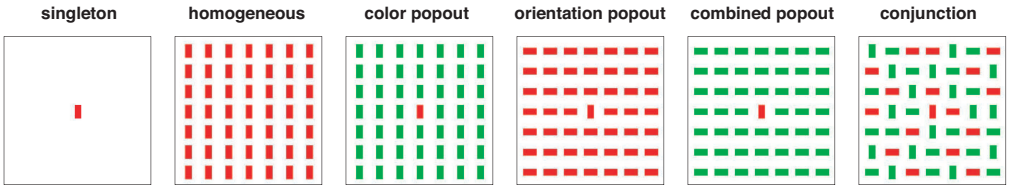

Figure S 1: The six different visual displays used in the experiments [1] and in our simulations. For convenience the target bar (red-vertical bar) in all displays is placed in the middle of the arrays.

References

[1] Burrows, B. E. & Moore, T. Influence and limitations of popout in the selection of salient visual stimuli by area V4 neurons. *J Neurosci* **29**, 15169–15177 (2009).

Table 1: Model parameters for simulations of saliency computations in successive layers

Symbol	Description	Value
	Network architectures	
	size of the visual fields	$14^\circ \times 14^\circ$
N_E	number of Exc neurons in each population	784 (28×28)
N_I	number of Inh neurons in each population	784 (28×28)
	number of populations in each layer	8
	number of layers	3
	total number of neurons	18816
	total number of synapses	$\approx 3.4 \times 10^7$
	Connectivity	
$\sigma_{EE,\ i\to i}$	width of connection from Exc to Exc neurons	0.5 degree
$\sigma_{EI,\ i\to i}$	width of connection from Exc to Inh neurons	1.0 degree
$\sigma_{IE,\ i\to i}$	width of connection from Inh to Exc neurons	1.5 degree
$\sigma_{II,\ i\to i}$	width of connection from Inh to Inh neurons	0.5 degree
$\sigma_{EE,\ i\to i+1}$	width of connection between layers	0.4 degree
	Connectivity strength	
$w^{AMPA}_{EE,\ i\to i}$	strength of connection for AMPA synapses	11
$w^{NMDA}_{EE,\ i\to i}$	strength of connection for NMDA synapses	44
$w^{AMPA}_{EI,\ i\to i}$	strength of connection for AMPA synapses	135
$w^{NMDA}_{EI,\ i\to i}$	strength of connection for NMDA synapses	90
$w^{GABA}_{IE,\ i\to i}$	strength of connection for GABA synapses	70
$w^{GABA}_{II,\ i\to i}$	strength of connection for GABA synapses	100
$w^{AMPA}_{EE,\ i\to i+1}$	strength of connection for AMPA synapses	21
$w^{NMDA}_{EE,\ i\to i+1}$	strength of connection for NMDA synapses	14

Exc = excitatory, Inh = inhibitory, $i \to i$ = connections from a population in layer i to corresponding locations in a population in layer i.

Table 2: Model parameters for simulations of the effect of feedback and the saccade preparation experiment

Symbol	Description	Value
	Network architectures	
	size of the visual fields	$14^\circ \times 14^\circ$
N_E	number of Exc neurons in each population	784 (28×28)
N_I	number of Inh neurons in each population	784 (28×28)
	total number of populations	10
	total number of neurons	7840
	total number of synapses	$\approx 2.7 \times 10^7$
	Connectivity	
$\sigma_{EE,\ F\to F}$	connection width for feature-selective neurons	0.7 degree
$\sigma_{EI,\ F\to F}$	connection width for feature-selective neurons	1.4 degree
$\sigma_{IE,\ F\to F}$	connection width for feature-selective neurons	0.7 degree
$\sigma_{II,\ F\to F}$	connection width for feature-selective neurons	2.0 degree
$\sigma_{EE,\ F\to S}$	connection width for feature-selective neurons	0.5 degree
$\sigma_{EI,\ F\to S}$	connection width for feature-selective neurons	1.5 degree
$\sigma_{EE,\ S\to F}$	connection width for saliency neurons	0.6 degree
$\sigma_{EI,\ S\to F}$	connection width for saliency neurons	1.5 degree
$\sigma_{EE,\ S\to S}$	connection width for saliency neurons	0.7 degree
$\sigma_{EI,\ S\to S}$	connection width for saliency neurons	1.4 degree
$\sigma_{IE,\ S\to S}$	connection width for saliency neurons	0.7 degree
$\sigma_{II,\ S\to S}$	connection width for saliency neurons	4.0 degree

continued on the next page

Table 2: Model parameters for simulations of the effect of feedback and the saccade preparation experiment (continuation)

Symbol	Description	Value
	Connectivity strength	
$w^{AMPA}_{EE,\ F\to F}$	strength of connection for AMPA synapses	17.5
$w^{NMDA}_{EE,\ F\to F}$	strength of connection for NMDA synapses	70
$w^{AMPA}_{EI,\ F\to F}$	strength of connection for AMPA synapses	270
$w^{NMDA}_{EI,\ F\to F}$	strength of connection for NMDA synapses	180
$w^{GABA}_{IE,\ F\to F}$	strength of connection for GABA synapses	120
$w^{GABA}_{II,\ F\to F}$	strength of connection for GABA synapses	160
$w^{AMPA}_{EE,\ F\to S}$	strength of connection for AMPA synapses	275
$w^{NMDA}_{EE,\ F\to S}$	strength of connection for NMDA synapses	165
$w^{AMPA}_{EI,\ F\to S}$	strength of connection for AMPA synapses	280
$w^{NMDA}_{EI,\ F\to S}$	strength of connection for NMDA synapses	80
$w^{AMPA}_{EE,\ S\to F}$	strength of connection for AMPA synapses	2.5
$w^{NMDA}_{EE,\ S\to F}$	strength of connection for NMDA synapses	1.5
$w^{AMPA}_{EI,\ S\to F}$	strength of connection for AMPA synapses	17.5
$w^{NMDA}_{EI,\ S\to F}$	strength of connection for NMDA synapses	5.0
$w^{AMPA}_{EE,\ S\to S}$	strength of connection for AMPA synapses	17.5
$w^{NMDA}_{EE,\ S\to S}$	strength of connection for NMDA synapses	70
$w^{AMPA}_{EI,\ S\to S}$	strength of connection for AMPA synapses	270
$w^{NMDA}_{EI,\ S\to S}$	strength of connection for NMDA synapses	180
$w^{GABA}_{IE,\ S\to S}$	strength of connection for GABA synapses	120
$w^{GABA}_{II,\ S\to S}$	strength of connection for GABA synapses	500

E = excitatory, I = inhibitory, F = feature-selective populations, S = saliency populations, $F \to S$ = connections from a feature-selective population to the corresponding locations in a saliency population.

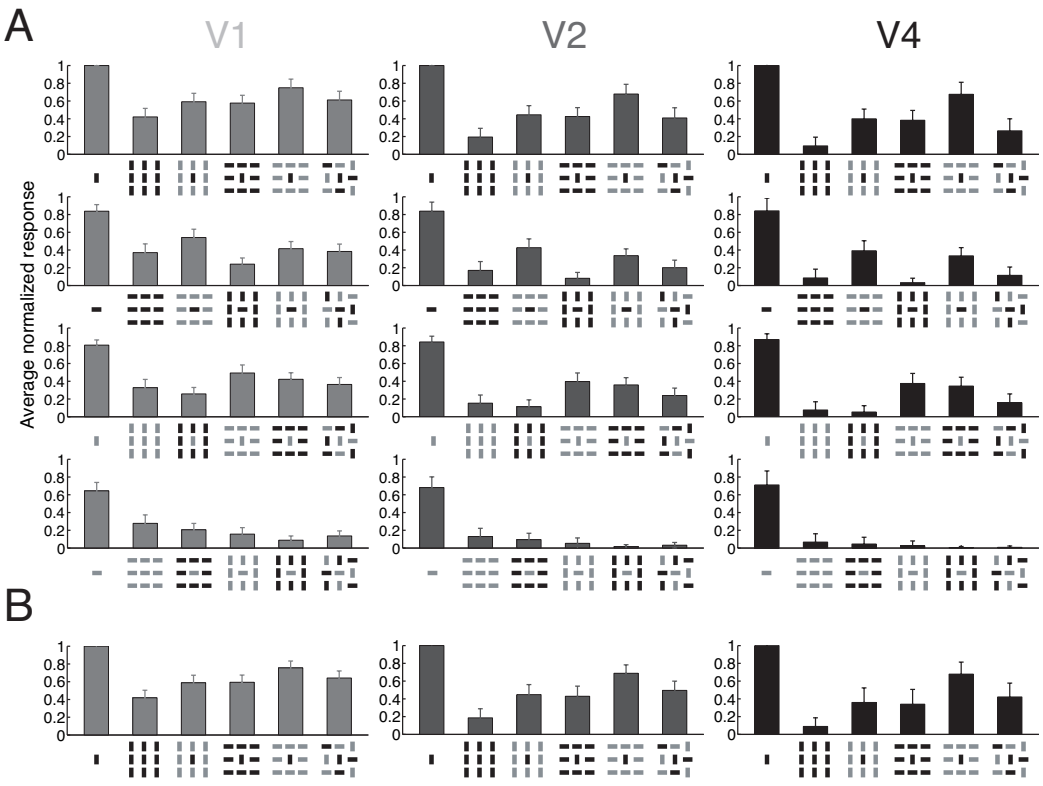

Figure S2: Average normalized response of target-selective neurons in V1, V2 and V4 to the 6 displays. The average normalized responses are computed by counting all spikes for 200 msec following the firing onset for 200 trials (see Fig. 2) and normalizing the sum by the response to the singleton display. Error bars show the standard deviation. The response to popout displays increases over that of the conjunction display only when individual features are processed separately (**A**) but not when they are combined (**B**).

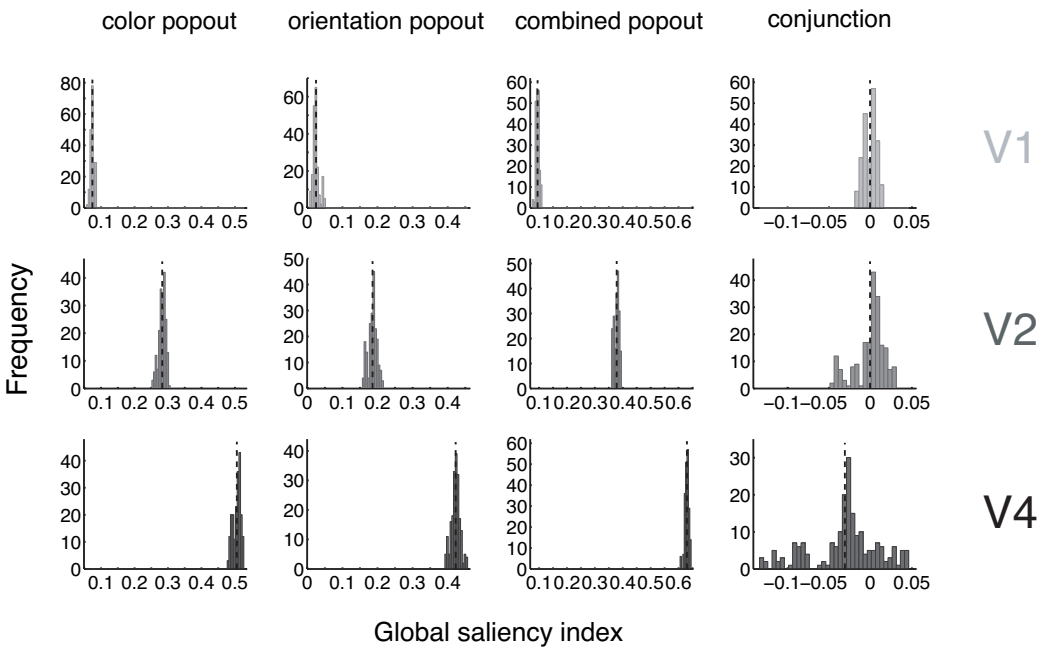

Figure S 3: Evolution of global saliency indices in successive layers of the network for configuration A. Histograms of global saliency index for popout and conjunction displays in successive layers of the network. Histogram of global saliency indices are computed from the average response in the first 200 msec of the visual response in 30 randomly selected trials. Dashed lines show the mean value for each histogram.

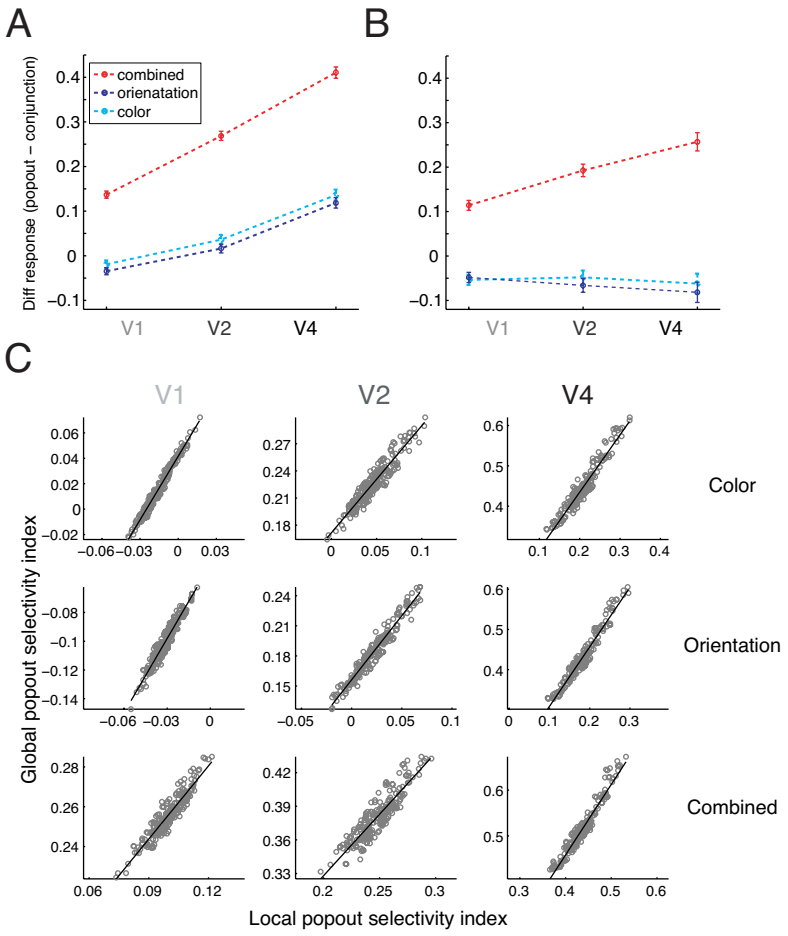

Figure S4: Local saliency signal increases in successive regions for configuration A and is correlated with the global saliency signal. (**A-B**) The difference between average response to different popout and conjunction displays are computed using average response of target-selective neurons in successive regions. Results for configurations A and B are shown in panels (A) and (B), respectively. Error bars show the s.e.m. The differential response increases in higher areas only for configuration A. (**C**) The global popout selectivity index, GPI, as a function of the local popout selectivity index, PI, for different popout displays and in different regions of the network in configuration A. Black lines show the linear fit in each case. These indices are computed using average response of neurons in 30 randomly selected trials. The local and global popout selectivity indices are strongly correlated in all regions and for all popout displays.

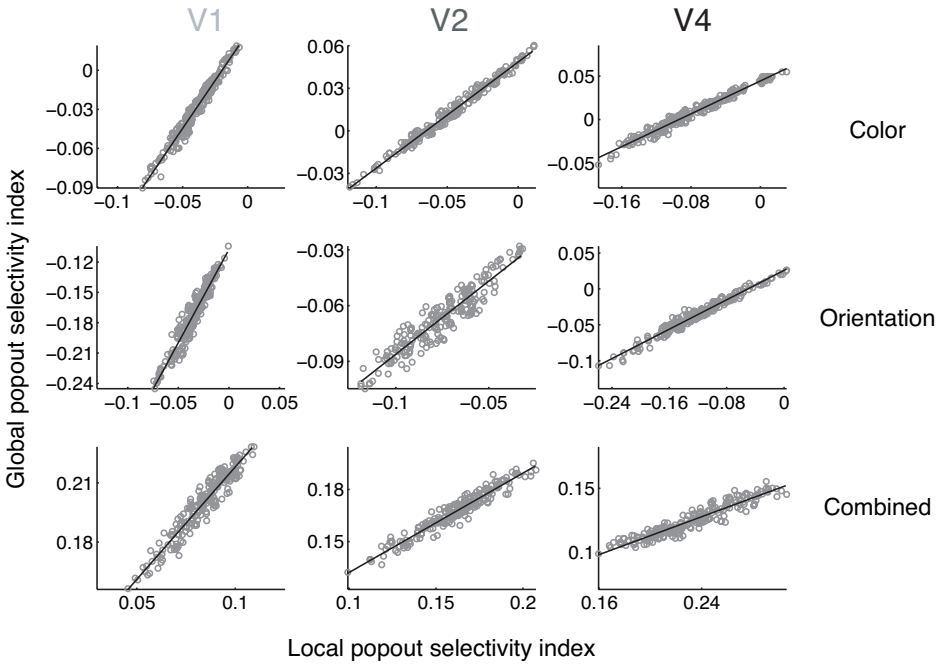

Figure S 5: Correlation between the global and local selectivity indices for configuration B. The global popout selectivity index, GPI, as a function of the local popout selectivity index, PI, for different popout displays and in different regions of the network. The global and local popout indices are strongly correlated in all regions and for all popout displays. Note that both the global and local popout indices have negative values for color and orientation popout in all three visual areas. These indices are computed using average response of neurons in 30 randomly selected trials. Black lines show the linear fit in each case.

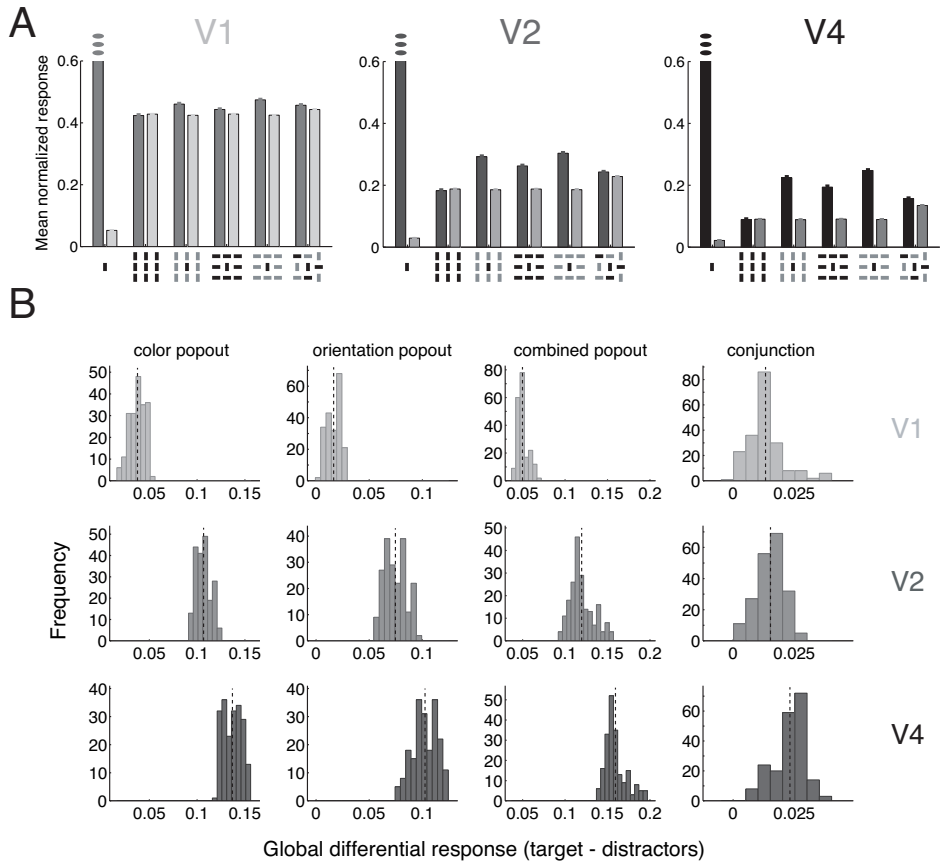

Figure S6: Evolution of the global saliency signal in successive regions for configuration B. (**A**) Average normalized response of the constructed saliency populations to different displays is plotted separately for neurons selective to either the target (central bar) or distractors (peripheral bars). The response of target-selective neurons is plotted with a darker shade than the response of distractor-selective neurons. The error bars are the s.e.m. For illustrative purposes, we only show the values of responses between 0 and 0.6 (the response to the single bar is equal to 1). The difference between the response to the target and distractors increases for popout displays while the overall response to the target decreases. (**B**) Histograms of the global differential response (*i.e.* the difference between response of target- and all distractor-selective neurons), for different displays. The dashed lines show the mean in each histogram. The differential response increases for both popout and conjunction displays in successive regions, but increases more greatly for popout displays.

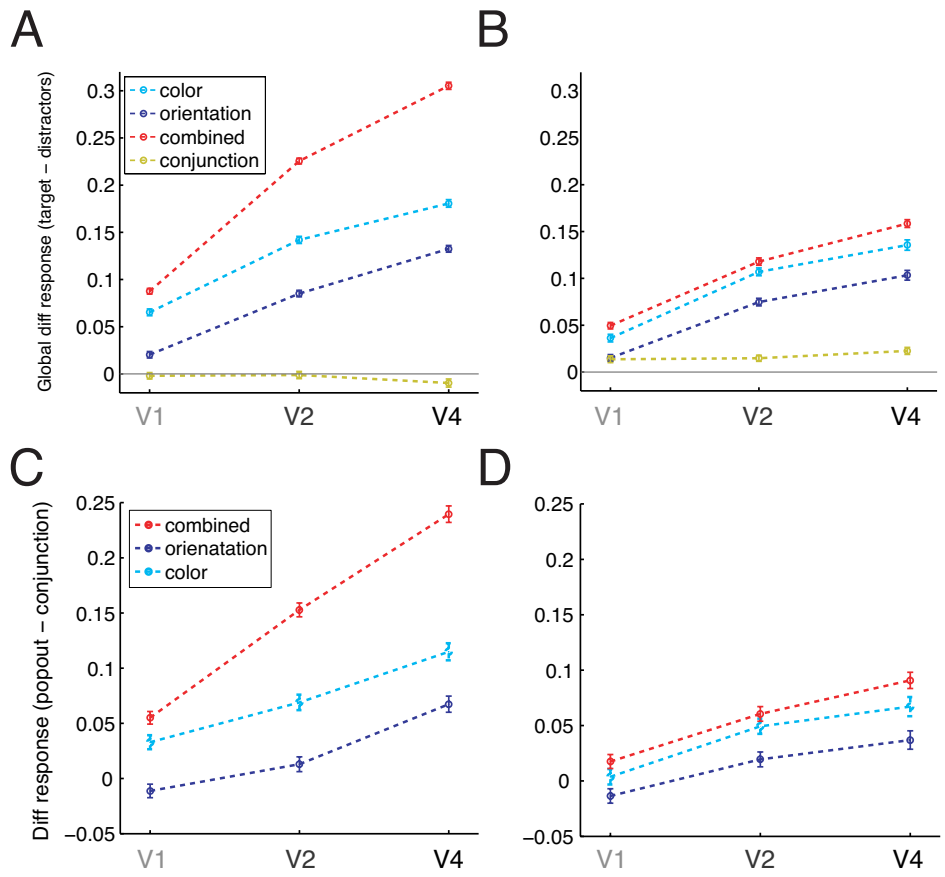

Figure S 7: Formation of the local and global saliency signals in the saliency population, in successive layers of the network and for the two configurations. The differential response of target-selective neurons in the constructed saliency populations is computed by adding the activity of all color- and/or orientation-selective neurons in each region. Results for configurations A and B are shown in panels (A) and (C), and (B) and (D), respectively. (**A-B**) The average global differential response (i.e. difference between response of target- and distractor-selective neurons), for different types of display and in successive regions of the network, for the constructed saliency populations. (**C-D**) The difference between average response to different popout and conjunction displays. These differences are computed using average response of target-selective neurons in successive regions. Overall, for configuration A, the differential response increases in successive regions more strongly. Error bars show the s.e.m.

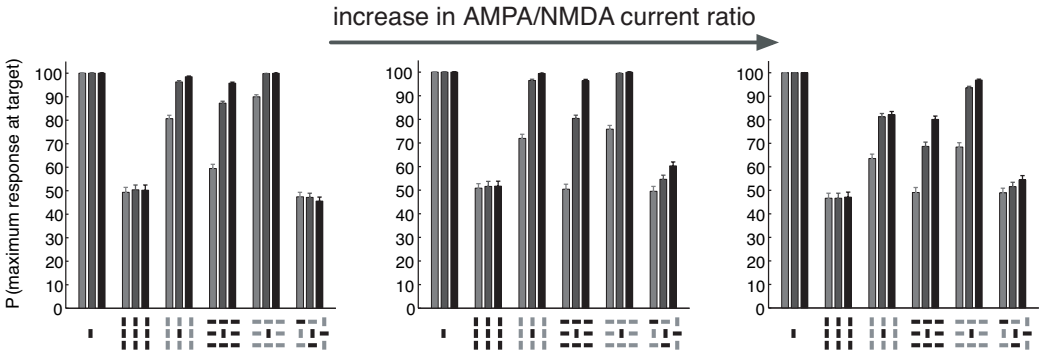

Figure S 8: Change in detection of the most salient location in successive regions of the network due to change in the AMPA to NMDA current ratio. The probability that the response of target selective neurons is the maximum response in the constructed saliency population is plotted with different shades of gray (light gray, medium gray, and black) corresponding to the three regions (V1, V2, and V4, respectively) for different displays. Results for different values of the AMPA to NMDA current ratios are shown in different panels.

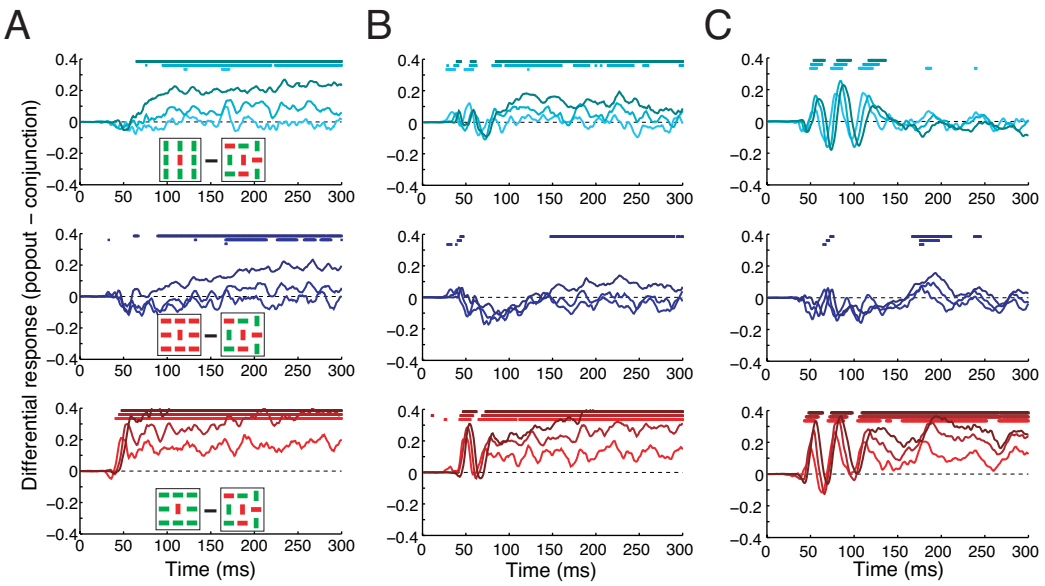

Figure S 9: Temporal dynamics of the local saliency signal in successive regions of the network and its dependence on the AMPA to NMDA current ratio. The difference in the normalized response to popout and conjunction displays is plotted for different types of popout display (indicated by insets) and for three visual areas of our model. Different shades of color (light to dark) correspond to response in successive regions (V1 to V4, respectively). The point at the top of each panel shows whether the differential response is statistically significant (at $p < 0.05$) for each 10 msec time interval. Results for larger values of the AMPA to NMDA current ratios are shown in panels (**A**) to (**C**), respectively. The larger AMPA to NMDA current ratio results in the delay and elimination of the local saliency signal formation for color and orientation popout displays, and in a stronger oscillatory response.

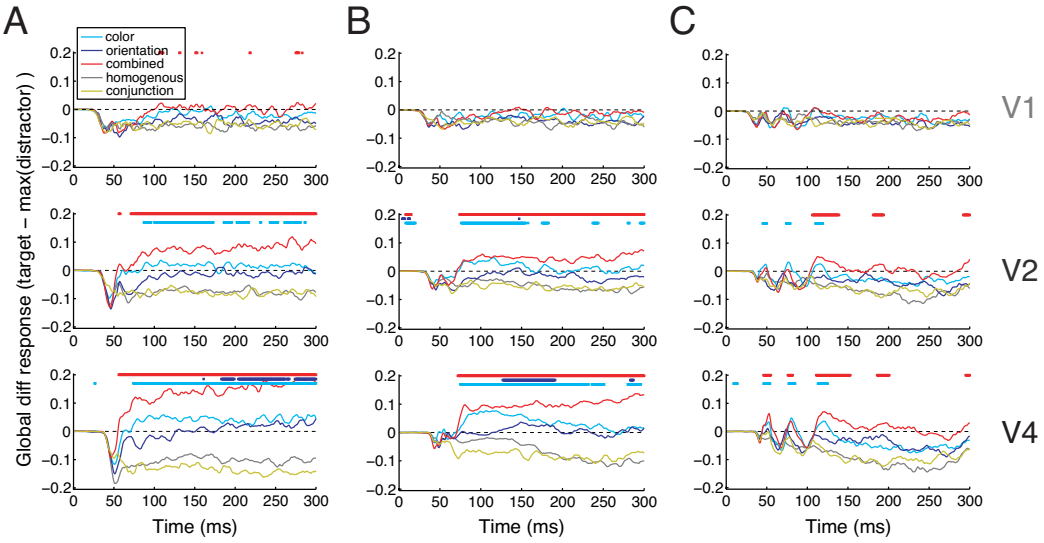

Figure S 10: Temporal dynamics of the global saliency signal in successive constructed saliency populations and its dependence on the AMPA to NMDA current ratio. The difference in the normalized response of neurons selective to the target and neurons selective to the distractor that exhibit the maximum activity in a given trial is plotted for different types of display (indicated in the inset). The point at the top of each panel shows whether the differential response is statistically significant (at $p < 0.05$) for each 10 msec time interval. Different regions corresponding to different visual areas are denoted at the right side of the sub-panels. Results for larger values of the AMPA to NMDA current ratio are shown in panels (**A**) to (**C**), respectively. A larger AMPA to NMDA current ratio results in the delay and elimination of the global saliency signal formation.

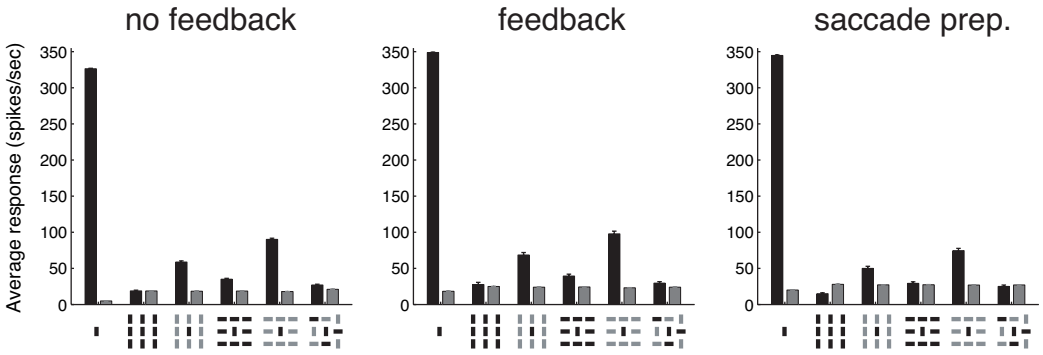

Figure S 11: The effect of feedback and saccade preparation on the response in the saliency map. Average response to different types of display is plotted separately for neurons selective to either the target (black) or distractors (gray) in three different cases: with no feedback, with feedback from the saliency map to all feature-selective populations, and simulated saccade preparation experiment. For the case with feedback, the difference between the response to the target and distractors is the largest and furthermore, the response to popout displays are more similar to each other and more different from the response to the conjunction display. During saccade preparation, the response to the target is reduced due to the high level of activity at the saccade target location, which also suppresses activity elsewhere in the saliency map population.